

Combined analysis of pion-induced reactions in a dynamical coupled-channels approach

M. Döring

**H. Haberzettl, J. Haidenbauer, C. Hanhart, F. Huang, S. Krewald,
U.-G. Meißner, K. Nakayama, D. Rönchen,**
Forschungszentrum Jülich, Universität Bonn, University of Georgia, GWU

The Jülich model of pion-nucleon interaction

Motivation

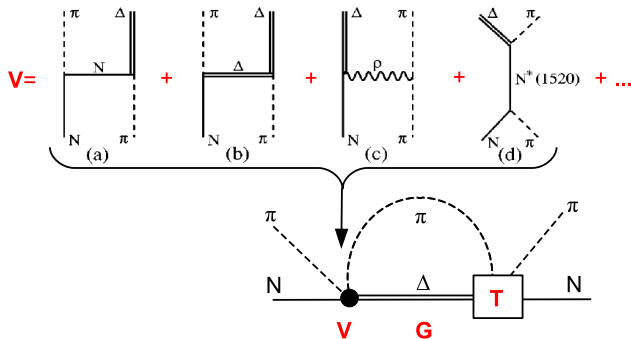
- Coupled channels πN , ηN , KY ; effective $\pi\pi N$ channels σN , ρN , $\pi\Delta$.
- Chiral Lagrangian of Wess and Zumino [PR163 (1967), Phys.Rept. 161 (1988)].
- Baryonic resonances up to $J = 7/2$ with derivative couplings.
- General requirements of the S -matrix.
 - Crossed (u -channel) contributions \rightarrow sub-threshold cuts.
 - Dispersive treatment of t -channel exchanges (σ , ρ exchange from $NN \rightarrow \pi\pi$).
 - Full analyticity, also of $\pi\pi N$ intermediate states \rightarrow additional branch points in complex plane.
 - 2-body unitarity, some requirements of 3-body unitarity (but not full).

Talks by S. Krewald, F. Huang

- Analytic structure and the "background", The reaction $\pi^+ p \rightarrow K^+ \Sigma^+$.
- Photoproduction.

Scattering equation in the JLS basis

$$\langle L' S' k' | T_{\mu\nu}^{IJ} | L S k \rangle = \langle L' S' k' | V_{\mu\nu}^{IJ} | L S k \rangle + \sum_{\gamma, L'' S''} \int_0^{\infty} k''^2 dk'' \langle L' S' k' | V_{\mu\gamma}^{IJ} | L'' S'' k'' \rangle \frac{1}{Z - E_{\gamma}(k'') + i\epsilon} \langle L'' S'' k'' | T_{\gamma\nu}^{IJ} | L S k \rangle$$



Scattering equation in the JLS basis

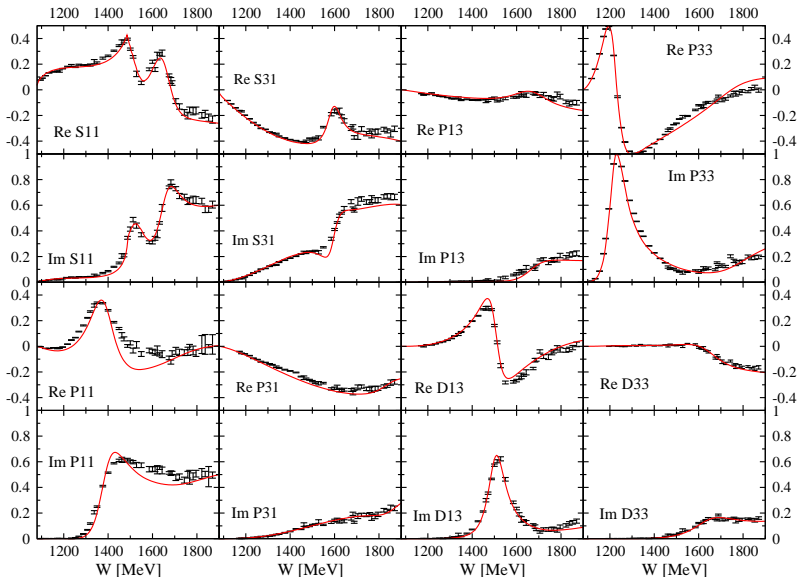
$$\langle L' S' k' | T_{\mu\nu}^{IJ} | L S k \rangle = \langle L' S' k' | V_{\mu\nu}^{IJ} | L S k \rangle + \sum_{\gamma, L'' S''} \int_0^{\infty} k''^2 dk'' \langle L' S' k' | V_{\mu\gamma}^{IJ} | L'' S'' k'' \rangle \frac{1}{Z - E_{\gamma}(k'') + i\epsilon} \langle L'' S'' k'' | T_{\gamma\nu}^{IJ} | L S k \rangle$$

Features

- Hadron exchange: provides the relevant dynamics.
- Full analyticity (dispersive parts).
- All partial waves are linked (t-, u-channel processes)
- Channels linked (SU(3) symmetry).
- Minimal resonance content required.
- Dynamical generation of resonances is possible, but not easy (strong constraints).

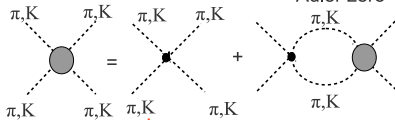
Partial waves in $\pi N \rightarrow \pi N$ (Solution 2002)

"Data": GWU/SAID, PRC74 (2006)

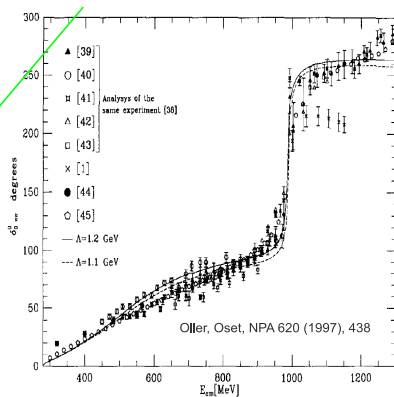
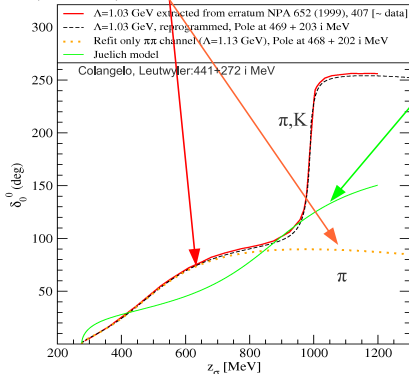
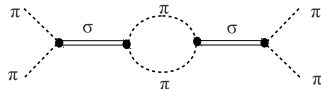


Example of chiral constraints: $\pi\pi$ scattering

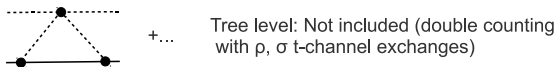
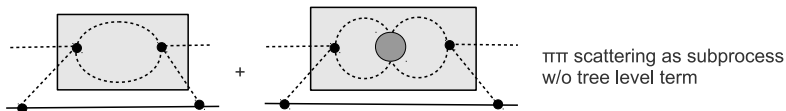
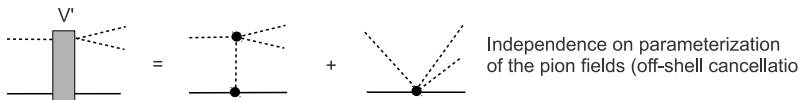
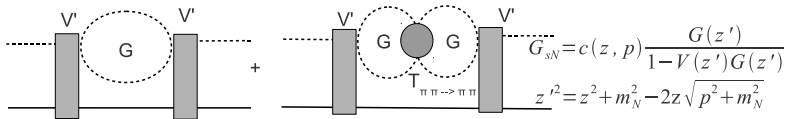
$$T_{\pi\pi} = V_\chi + V_\chi G T_{\pi\pi}; \quad V_\chi = \underbrace{(1/2m_\pi^2 - s)}_{\text{Adler zero}} / f^2$$



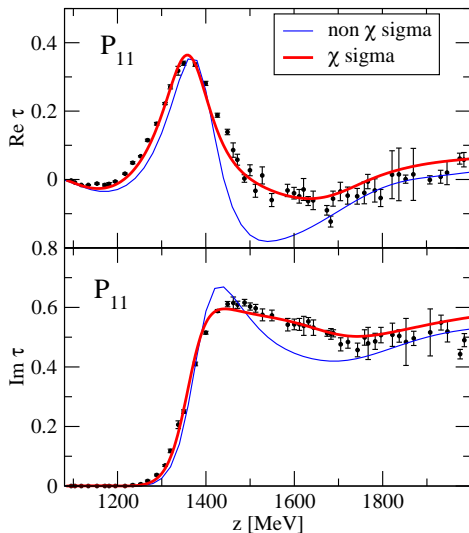
$$T_{\pi\pi} = (V_{\sigma\pi\pi})^2 / (z - M - \Sigma_{\pi\pi})$$



Implementation of the chiral σ



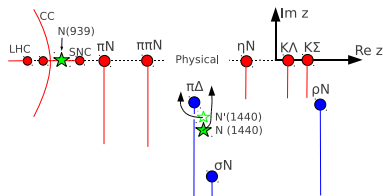
Effects of the χ unitary σ meson in the P_{11} πN amplitude



- Dynamical generation of Roper does not depend on details of the model
- Chiral σ provides better description.

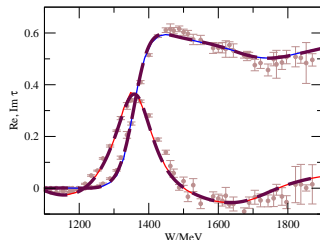
Structure of the P11 partial wave (Roper)

analytic continuation



- σN interaction strongly attractive \rightarrow dynamical generation of the Roper.
- Roper pole + $\pi\Delta$ branch point \rightarrow non-standard resonance shape.

- Where is the $3^* N(1710)$?
[S. Ceci, M.D. et al, arXiv 1104.3490]



Fit of a model without ρN branch point (CMB type) [solid lines] to the Jülich amplitude [dashed lines]

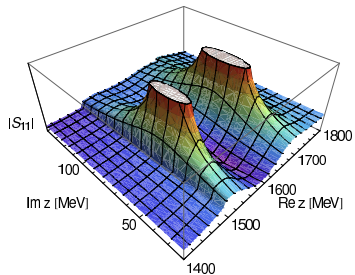
- CMB fit to JM has pole at $1698 - 130 i$ MeV, simulates missing branch point.

Branch points in $\gamma n \rightarrow \eta n$

Inclusion of full analytic structure important to avoid false pole signals.

Poles and residues

[M.D., C. Hanhart, F. Huang, S. Krewald and U.-G. Meißner, NPA 829 (2009), PLB 681 (2009)]



	Re z_0 [MeV]	-2 Im z_0 [MeV]	$ R $ [MeV]	θ [deg] [$^{\circ}$]	
$N^*(1535) S_{11}$	1519	129	31	-3	
ARN	1502	95	16	-16	
HOE	1487				
CUT	1510±50	260±80	120±40	+15±45	
$N^*(1650) S_{11}$	1669	136	54	-44	
ARN	1648	80	14	-69	
HOE	1670	163	39	-37	
CUT	1640±20	150±30	60±10	-75±25	
$N^*(1720) P_{13}$	1663	212	14	-82	
ARN	1666	355	25	-94	
HOE	1686	187	15		
CUT	1680±30	120±40	8±12	-160±30	
$\Delta(1232) P_{33}$	1218	90	47	-37	
ARN	1211	99	52	-47	
HOE	1209	100	50	-48	
CUT	1210±1	100±2	53±2	-47±1	
$\Delta^*(1620) S_{31}$	1593	72	12	-108	
ARN	1595	135	15	-92	
HOE	1608	116	19	-95	
CUT	1600±15	120±20	15±2	-110±20	
$N^*(1440) P_{11}$	1387	147	48	-64	$\Delta^*(1700) D_{33}$
ARN	1359	162	38	-98	ARN
HOE	1385	164	40		HOE
CUT	1375±30	180±40	52±5	-100±35	CUT
$N^*(1520) D_{13}$	1505	95	32	-18	$\Delta^*(1910) P_{31}$
ARN	1515	113	38	-5	ARN
HOE	1510	120	32	-8	HOE
CUT	1510±5	114±10	35±2	-12±5	CUT

[ARN]: Arndt et al., PRC 74 (2006), [HOE]: Höhler, πN Newsl. 9 (1993), [CUT]: Cutkowski et al., PRD 20 (1979).

Residues to ηN , σN , ρN , $\pi \Delta$. Zeros. Branching ratios to πN , ηN .

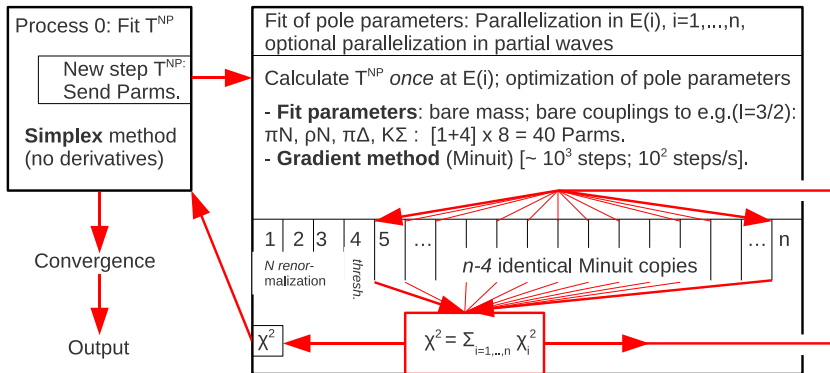
Parallelization

[Project *JIKP07* on JUROPA/FZ Jülich, 384,000 CPU hours granted]

Fixing free parameters from s-channel "pole" processes [fast!] and t -, u - processes [$\sim 100 \times$ slower]

Requirements:

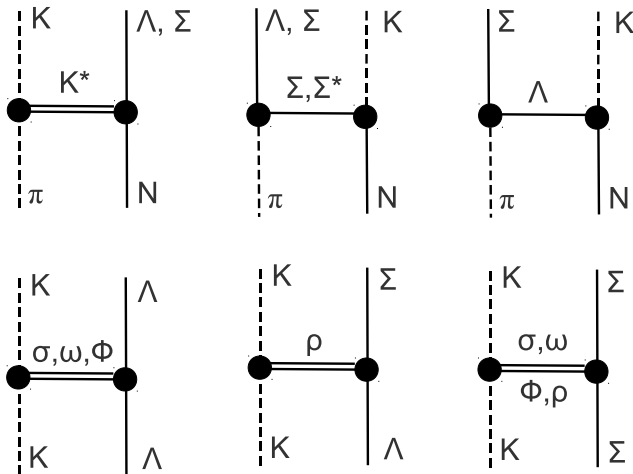
- 1) Maintain speed advantage of ($\times 100$) of calculation of T^P from T^{NP} ($T=T^{NP}+T^P$)
 - > 2 nested Minuit runs: full fit of T^P [-40 parms.] for every step in T^{NP}
 - > requires separated memory spaces/ **mpi** parallelization on **Juropa/FZ Julich**
- 2) Scaling with # processes
- 3) Adding large amounts of data to χ^2 without increase of execution time



Inclusion of the KY channels

[see talk S. Krewald]

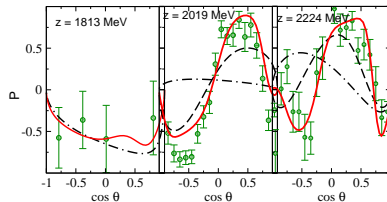
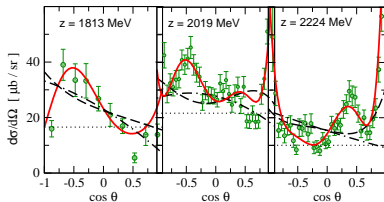
Inclusion via $SU(3)$ symmetry **plus s -channel resonance vertices to KY (not shown; 40 parms.)**.



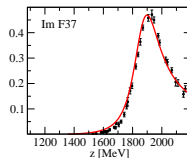
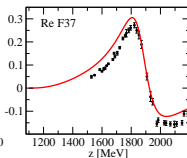
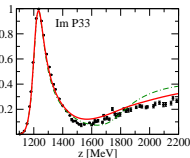
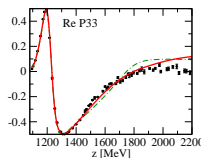
The reaction $\pi^+ p \rightarrow K^+ \Sigma^+$

M.D., C. Hanhart, F. Huang, S. Krewald, U.-G. Meißner, D. Rönchen, [NPA851 (2011)]

[Link to full Results & Error analysis](#)



Data upper: Candlin 1983, NPB 226 (1983), lower: GWU/SAID, PRC74 (2006)



Linking partial waves and **different reactions** puts more constraints on

resonance content

Pole Structure of the Amplitudes

extracted from analytic continuation

[Nucl.Phys.A851:58-98,2011]

Established 4-star resonances:

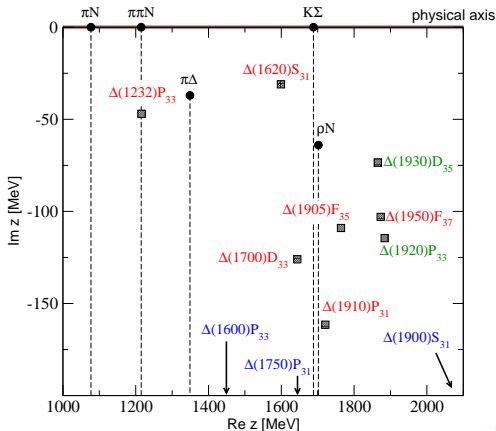
$\Delta(1232)P_{33}$, $\Delta(1700)D_{33}$,
 $\Delta(1905)F_{35}$, $\Delta(1950)F_{37}$,
 $\Delta(1620)S_{31}$, $\Delta(1910)P_{31}$

3-star resonances:

$\Delta(1920)P_{33}$, $\Delta(1930)D_{35}$
constraints from $K^+\Sigma^+$ data lead to
positions in vicinity of 3-star PDG
resonances

Dynamically generated poles:

$\Delta(1600)P_{33}$



Comparison of poles (extracted from $\pi N \rightarrow \pi N$ & $\pi^+ \rightarrow K^+\Sigma^+$)

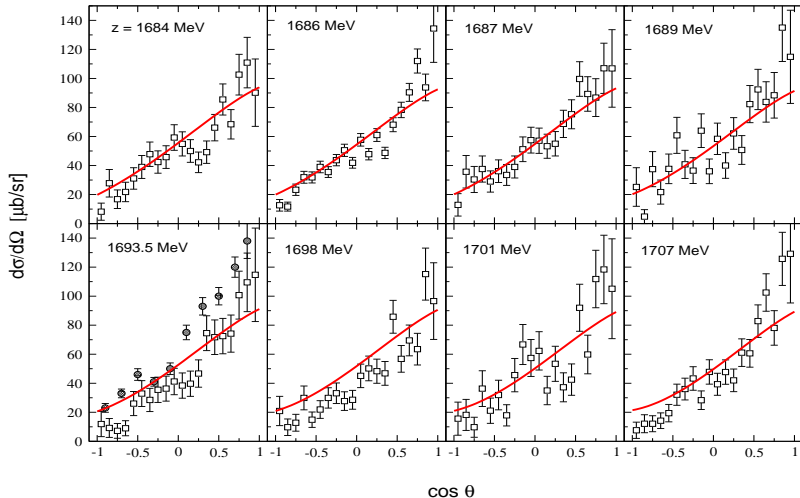
Data:	$\pi N + K^+\Sigma^+ (+\dots)$		πN					$K^+\Sigma^+$	$\pi\pi N$	Quark Models	
Analysis:	Jülich	Gießen	GWU	KH	CMB	EBAC	DMT	Cdl	Mnly	LMP, A	CI
Type:	DCM	KM	KM/DA	DA	DA	DCM	DCM	IA	KM	-	-
Pole/BW:	P	BW	P	SP	P	P	P	BW	BW	-	-
$\Delta(1232)P_{33}$	1216	1228(1)	1211	1209	1210	1211	1212	-	1232	1261	1230
$3/2^+ ****$	96	106(1)	99	100	100	100	98	-	118	-	-
$\Delta(1600)P_{33}$	1455 ^(a)	1667(1)	1457	1550	1550	-	1544	-	1706	1810	1795
$3/2^+ ***$	694	397(10)	400	-	200	-	190	-	430	-	-
$\Delta(1620)S_{31}$	1599	1612(2)	1595	1608	1600	1563	1589	-	1672	1654	1555
$1/2^- ****$	62	202(7)	135	116	120	190	148	-	154	-	-
$\Delta(1700)D_{33}$	1644	1678(1)	1632	1651	1675	1604	1604	-	1762	1628	1620
$3/2^- ****$	252	606(15)	253	159	220	212	142	-	599	-	-
$K^+\Sigma^+(1688)$											
$\Delta(1750)P_{31}$	1668 ^(a)	1712(1)	1771	-	-	-	-	-	1744	1866	-
$1/2^+ *$	892	643(17)	479	-	-	-	-	-	299	-	-
$\Delta(1900)S_{31}$	-	1984	-	1780	1870	-	1774	-	1920	2100	2035
$1/2^- **$		237		170	180		72		263	-	-
$\Delta(1905)F_{35}$	1764	1845(15)	1819	1829	1830	1738	1760	1960	1881	1897	1910
$5/2^+ ****$	218	426(26)	247	303	280	220	200	270	327	-	-
$\Delta(1910)P_{31}$	1721	1975	1771	1874	1880	-	1900	-	1882	1906	1875
$1/2^+ ****$	323	676	479	283	200	-	174	-	239	-	-
$\Delta(1920)P_{33}$	1884	2057(1)	-	1900	1900	-	-	1840	2014	1871	1915
$3/2^+ ***$	229	525(32)	-	-	300	-	300	200	152	-	-
$\Delta(1930)D_{35}$	1865	-	2001	1850	1890	-	1989	-	1956	2179	2155
$5/2^- ***$	147	-	387	180	260	-	280	-	526	-	-
$\Delta(1940)D_{33}$	-	-	-	-	-	-	-	-	2057	2089	2080
$3/2^- *$									460	-	-
$\Delta(1950)F_{37}$	1873	-	1876	1878	1890	1858	1858	1925	1945	1956	1940
$7/2^+ ****$	206	-	227	230	260	200	208	330	300	-	-



Example of other final states [preliminary, no $N(1710)P11$ needed so far]

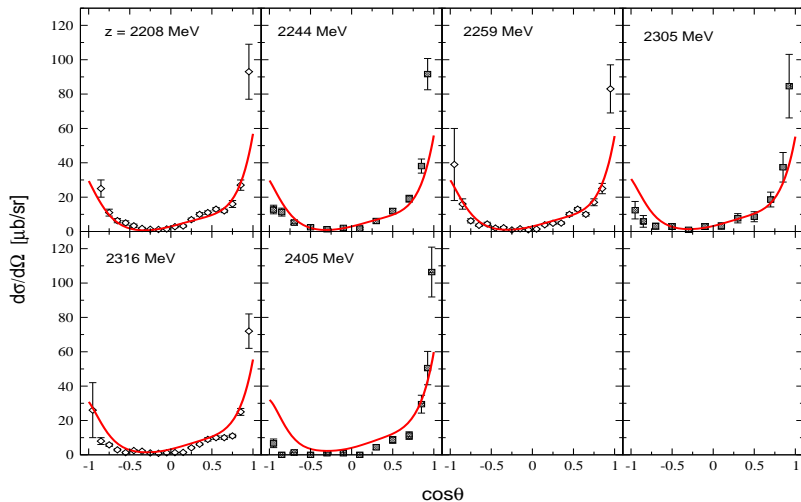
$$\pi^- p \rightarrow K^0 \Lambda$$

- Knasel 75, PRD 11,1
- Baker 78, NPB 141,29



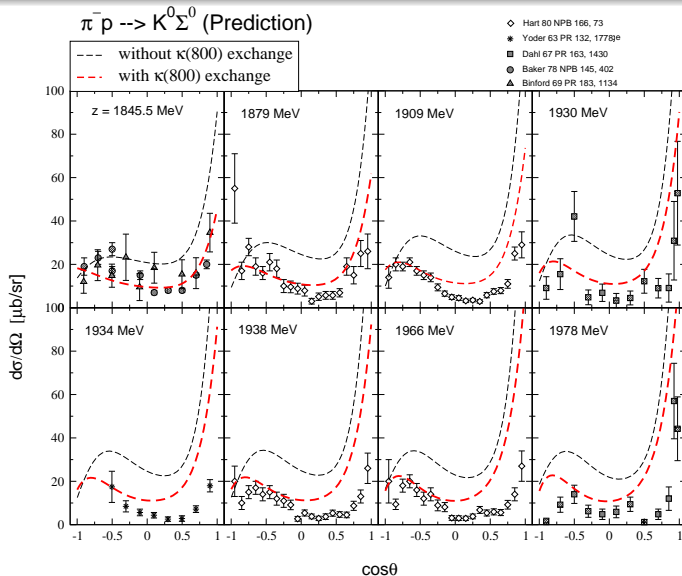
$$\pi^- p \rightarrow K^0 \Lambda$$

- ◇ Saxon 80, NPB 162, 522
- Dahl 67, PR 163, 1430



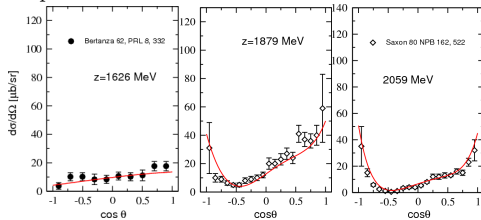
The power of SU(3)

Fixing u -, t -channel exchanges from $\pi N \rightarrow \pi N, K^+\Sigma^+, K^0\Lambda, \eta N$

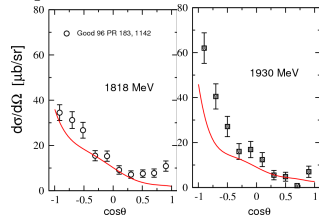


First results other KY channels: differential cross section

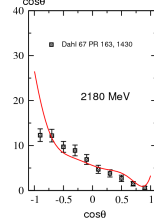
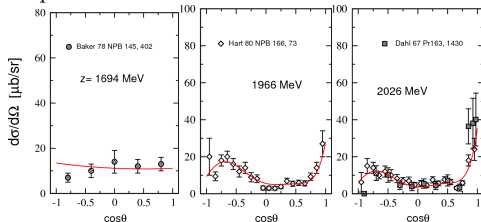
$$\pi^- p \rightarrow K^0 \Lambda:$$



$$\pi^- p \rightarrow K^+ \Sigma^-:$$

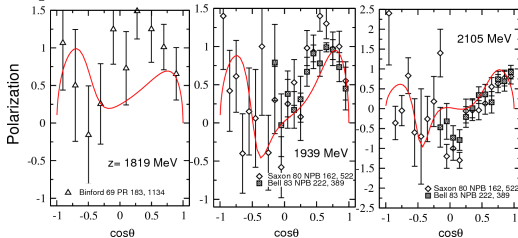


$$\pi^- p \rightarrow K^0 \Sigma^0:$$

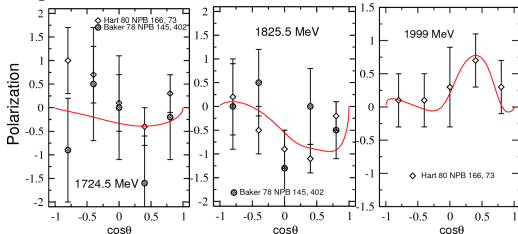


First results other KY channels: Polarization

$$\pi^- p \rightarrow K^0 \Lambda:$$



$$\pi^- p \rightarrow K^0 \Sigma^0:$$



$$\pi^- p \rightarrow K^+ \Sigma^-:$$

no data

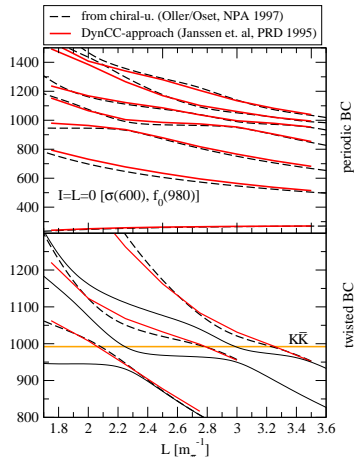
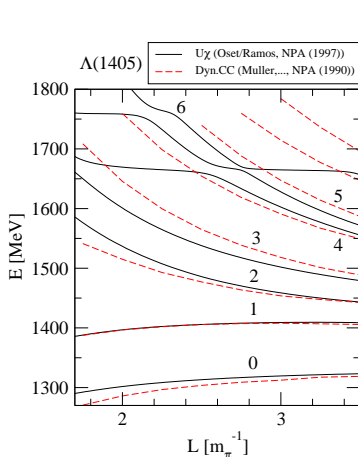
- HADES proposal: Measurement of π^- induced reactions
HADES Symp., May 13, 2011, Seillac, France.
- c.m. energies from 1.7 to 2 GeV.
- Additional motivation most welcome!

Dynamical coupled channels models in a box

Discretization & twisted BC

[M.D., J. Haidenbauer, A. Rusetsky, U.-G. Meißner, E. Oset, in preparation]

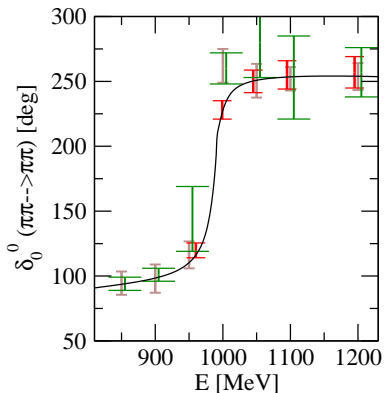
- Variation of box size $L \rightarrow$ reconstruction of phase shifts (Lüscher)
- Prediction of lattice levels & including coming lattice-data in analysis.
- Examples: $\Lambda(1405)$, $\sigma(600)$, $f_0(980)$ on the lattice.



Multi-channel dynamics

Error propagation from pseudo lattice-data [M.D., U.-G. Meißner, E. Oset, A. Rusetsky, in prep.]

- Coupled channels $\pi\pi, \bar{K}K$:
 three unknowns
 - $V(\pi\pi \rightarrow \pi\pi)$
 - $V(\pi\pi \rightarrow \bar{K}K)$
 - $V(\bar{K}K \rightarrow \bar{K}K)$
- How good is the reconstructed phase shift using different lattice data?
- Use pseudo-data generated from hadronic model.
- Hadronic input can reduce the error.



- red: twisted boundary conditions
- green: Asymmetric boxes
- brown: different levels

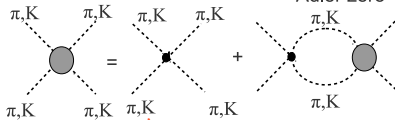
Conclusions

- Meson and baryon exchange: relevant degrees of freedom in the 2nd and 3rd resonance region.
- Exchange provides constraints, because all **partial waves & reactions** are linked \rightarrow minimal resonance content.
- Lagrangian based, field theoretical description of meson-baryon interaction. Unitarity and analyticity are ensured.
- Constructed to fulfill general requirements of the S -matrix (dispersive t -, u -channel [crossing]), branch points in complex plane, \dots
- \Rightarrow precise determination of model independent resonance parameters (poles).
- Parallelization & program structure: Inclusion of large amounts of data possible.
- Dynamical coupled channel models on a momentum lattice: predict levels, error propagation, analyse coming lattice data.

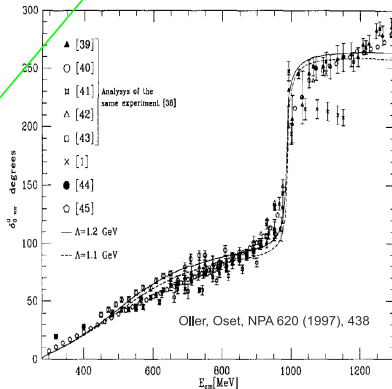
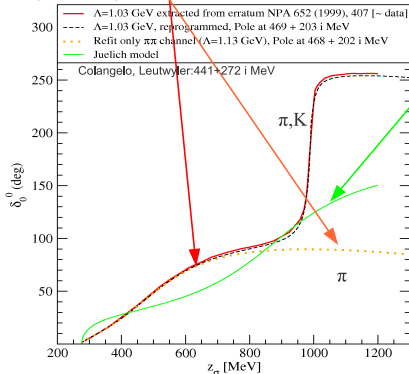
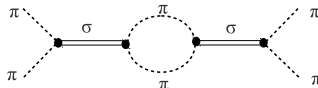


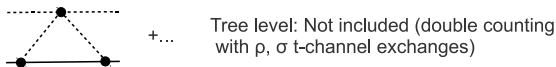
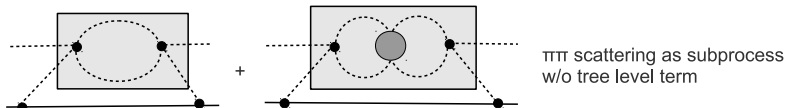
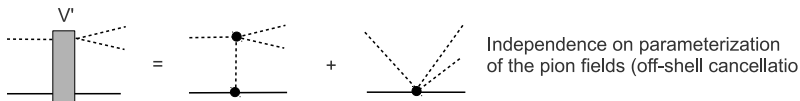
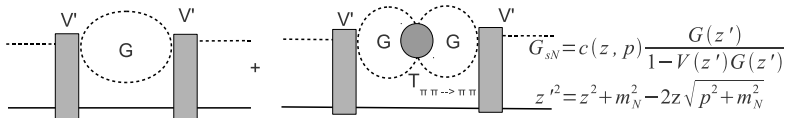
Chiral unitary approach to $\pi\pi$ scattering

$$T_{\pi\pi} = V_\chi + V_\chi G T_{\pi\pi}; \quad V_\chi = \underbrace{(1/2m_\pi^2 - s)}_{\text{Adler zero}} / f^2$$



$$T_{\pi\pi} = (V_{\sigma\pi\pi})^2 / (z - M - \Sigma_{\pi\pi})$$





Analytic continuation via Contour deformation

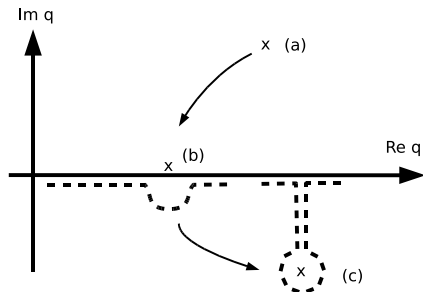
...enables access to all Riemann sheets

$$\Pi_{\sigma}(z) = \int_0^{\infty} q^2 dq \frac{(v^{\sigma\pi\pi}(q))^2}{z - E_1 - E_2 + i\epsilon}$$

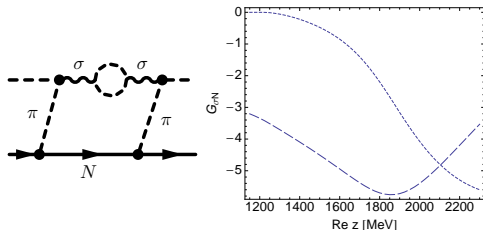
$$z - E_1 - E_2 = 0 \Leftrightarrow q = q_{c.m.}$$

$$q_{c.m.} = \frac{1}{2z} \sqrt{[z^2 - (m_1 - m_2)^2][z^2 - (m_1 + m_2)^2]}$$

- Plot $q_{c.m.}(z)$ in the q plane of integration (X: Pole positions).
- case (a), $\text{Im } z > 0$: straight integration from $q = 0$ to $q = \infty$.
- case (b), $\text{Im } z = 0$: Pole is on real q axis.
- case (c), $\text{Im } z < 0$: Deformation gives analytic continuation.
- Special case: Pole at $q = 0$
 \Leftrightarrow branch point at $z = m_1 + m_2$ (= threshold).



Propagator of effective $\pi\pi N$ channels σN , ρN , $\pi\Delta$

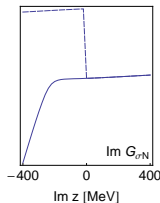
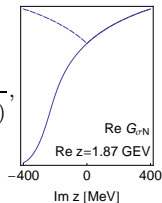
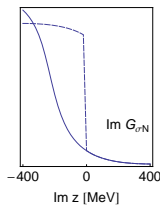
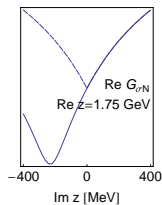


$$g_{\sigma N}(z, k) =$$

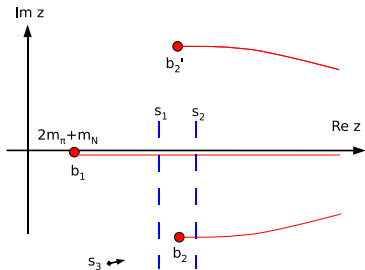
$$\frac{1}{z - \sqrt{m_N^2 + k^2} - \sqrt{(m_\sigma^0)^2 + k^2} - \Pi_\sigma(z_\sigma(z, k), k)},$$

$$G_{\sigma N}(z) = \int_0^\infty dk k^2 F(k) g_{\sigma N}(z, k),$$

$$z_\sigma(z, k) = z + m_\sigma^0 - \sqrt{k^2 + (m_\sigma^0)^2} - \sqrt{k^2 + m_N^2}$$



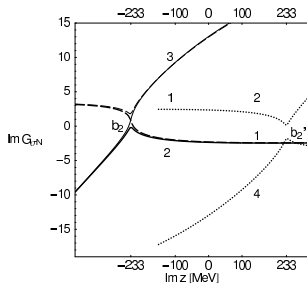
→ Branch point in the complex z plane.

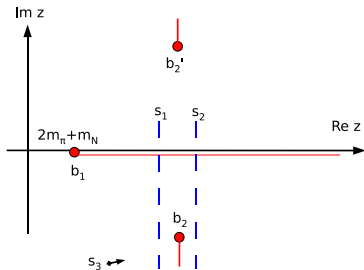


Three branch points and four sheets for each of the σN , ρN , and $\pi\Delta$ propagators.

- The cut along $\text{Im } z = 0$ is induced by the cut of the self energy of the unstable particle.
- The poles of the unstable particle (σ) induce branch points in the σN propagator at

$$z_{b_2} = m_N + z_0, \quad z_{b_2'} = m_N + z_0^*$$

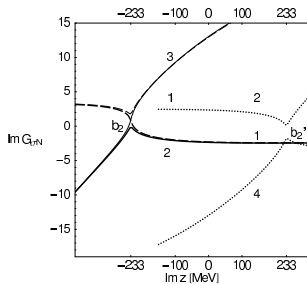


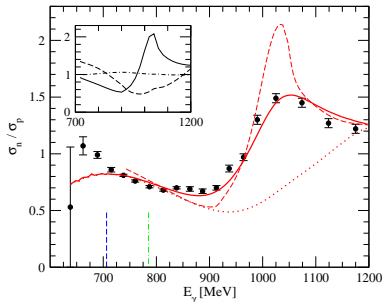


Three branch points and four sheets for each of the σN , ρN , and $\pi\Delta$ propagators.

- The cut along $\text{Im } z = 0$ is induced by the cut of the self energy of the unstable particle.
- The poles of the unstable particle (σ) induce branch points in the σN propagator at

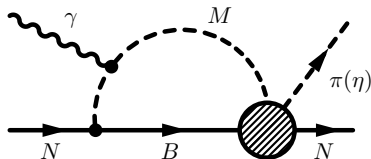
$$z_{b_2} = m_N + z_0, \quad z_{b_2'} = m_N + z_0^*$$



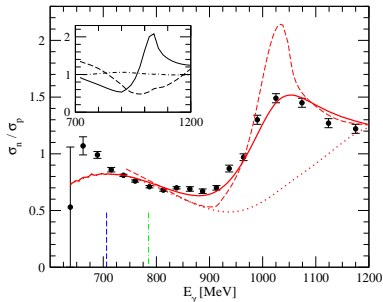


[Data: I. Jaegle et al., CBELSA/TAPS, PRL 100 (2008)]

- Intermediate states in photon loops, $Q = 0, 1$:
- $\pi^- p, \pi^0 n, \eta n, K^0 \Lambda, K^+ \Sigma^-, K^0 \Sigma^0$
- $\pi^0 p, \pi^+ n, \eta p, K^+ \Lambda, K^+ \Sigma^0, K^0 \Sigma^+$

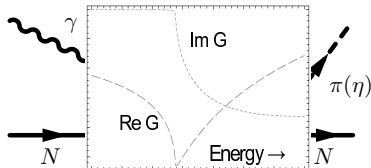


- Pronounced cusp from dispersive ("real") part of the loop.
- Peak in σ_n/σ_p : Direkt consequence of Weinberg-Tomozawa driving term from LO χ Lagrangian.



[Data: I. Jaegle et al., CBELSA/TAPS, PRL 100 (2008)]

- Intermediate states in photon loops, $Q = 0, 1$:
- $\pi^- p, \pi^0 n, \eta n, K^0 \Lambda, K^+ \Sigma^-, K^0 \Sigma^0$
- $\pi^0 p, \pi^+ n, \eta p, K^+ \Lambda, K^+ \Sigma^0, K^0 \Sigma^+$



- Pronounced cusp from dispersive ("real") part of the loop.
- Peak in σ_n/σ_p : Direkt consequence of Weinberg-Tomozawa driving term from LO χ Lagrangian.

	$N\pi$	$N\rho^{(1)} (S = 1/2)$	$N\rho^{(2)} (S = 3/2)$	$N\rho^{(3)} (S = 3/2)$
$N^*(1535) S_{11}$	$S_{11} \quad 8.1 + 0.5i$	$S_{11} \quad 2.2 - 5.4i$	–	$D_{11} \quad 0.5 - 0.5i$
$N^*(1650) S_{11}$	$S_{11} \quad 8.6 - 2.8i$	$S_{11} \quad 0.9 - 9.1i$	–	$D_{11} \quad 0.3 - 0.3i$
$N^*(1440) P_{11}$	$P_{11} \quad 11.2 - 5.0i$	$P_{11} \quad -1.3 + 3.2i$	$P_{11} \quad 3.6 - 2.6i$	–
$\Delta^*(1620) S_{31}$	$S_{31} \quad 2.9 - 3.7i$	$S_{31} \quad 0.0 - 0.0i$	–	$D_{31} \quad 0.0 - 0.0i$
$\Delta^*(1910) P_{31}$	$P_{31} \quad 1.2 - 3.5i$	$P_{31} \quad 0.2 - 0.4i$	$P_{31} \quad -0.2 - 0.4i$	–
$N^*(1720) P_{13}$	$P_{13} \quad 3.7 - 2.6i$	$P_{13} \quad 0.1 + 0.8i$	$P_{13} \quad -1.1 + 0.1i$	$F_{13} \quad 0.1 - 0.1i$
$N^*(1520) D_{13}$	$D_{13} \quad 8.4 - 0.8i$	$D_{13} \quad -0.6 + 0.7i$	$D_{13} \quad 0.9 - 2.0i$	$S_{13} \quad -2.5 - 0.5i$
$\Delta(1232) P_{33}$	$P_{33} \quad 17.9 - 3.2i$	$P_{33} \quad -1.3 - 0.8i$	$P_{33} \quad -0.9 - 3.0i$	$F_{33} \quad 0.0 - 0.0i$
$\Delta^*(1700) D_{33}$	$D_{33} \quad 4.9 - 1.0i$	$D_{33} \quad -0.2 + 0.9i$	$D_{33} \quad -0.4 - 0.4i$	$S_{33} \quad -0.1 - 0.1i$

	$N\eta$	$\Delta\pi^{(1)}$	$\Delta\pi^{(2)}$	$N\sigma$
$N^*(1535) S_{11}$	$S_{11} \quad 11.9 - 2.3i$	–	$D_{11} \quad -5.9 + 4.8i$	$P_{11} \quad -1.4 - 1.4i$
$N^*(1650) S_{11}$	$S_{11} \quad -3.0 + 0.5i$	–	$D_{11} \quad 4.3 + 0.4i$	$P_{11} \quad -2.1 - 2.1i$
$N^*(1440) P_{11}$	$P_{11} \quad -0.1 + 0.0i$	$P_{11} \quad -4.6 - 1.7i$	–	$S_{11} \quad -8.3 - 8.3i$
$\Delta^*(1620) S_{31}$	–	–	$D_{31} \quad 11.1 - 4.0i$	–
$\Delta^*(1910) P_{31}$	–	$P_{31} \quad 15.0 - 0.3i$	–	–
$N^*(1720) P_{13}$	$P_{13} \quad -7.7 + 5.5i$	$P_{13} \quad -14.1 + 3.0i$	$F_{13} \quad 0.0 - 0.3i$	$D_{13} \quad -0.8 - 0.8i$
$N^*(1520) D_{13}$	$D_{13} \quad 0.16 - 0.60i$	$D_{13} \quad 0.0 + 0.4i$	$S_{13} \quad -12.9 - 0.7i$	$P_{13} \quad -0.6 - 0.6i$
$\Delta(1232) P_{33}$	–	$P_{33} \quad -(4 \text{ to } 5) + i(0 \text{ to } 0.5)$	$F_{33} \quad \sim 0$	–
$\Delta^*(1700) D_{33}$	–	$D_{33} \quad -0.7 - 0.3i$	$S_{33} \quad -19.7 + 4.5i$	–

Resonance couplings g_i [$10^{-3} \text{ MeV}^{-1/2}$] to the coupled channels i . Also, the LJS type of each coupling is indicated. For the ρN channels, the total spin S is also indicated.

first sheet	second sheet	[FA02]
P_{11} 1235 - 0 i	S_{11} 1587 - 45 i	1578 - 38 i
D_{33} 1396 - 78 i	S_{31} 1585 - 17 i	1580 - 36 i
	P_{31} 1848 - 83 i	1826 - 197 i
	P_{13} 1607 - 38 i	1585 - 51 i
	P_{33} 1702 - 64 i	-
	D_{13} 1702 - 64 i	1759 - 64 i

Position of **zeros** of the full amplitude T in [MeV]. [FA02]: Arndt et al., PRC 69 (2004).

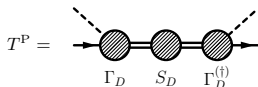
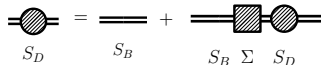
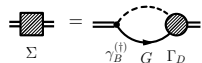
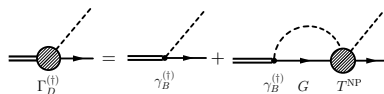
	$\Gamma_{\pi N}/\Gamma_{\text{Tot}}$ [%]	$\Gamma_{\eta N}/\Gamma_{\text{Tot}}$ [%]
$N^*(1535) S_{11}$	48 [33 to 55]	38 [45 to 60]
$N^*(1650) S_{11}$	79 [60 to 95]	6 [3 to 10]
$N^*(1440) P_{11}$	64 [55 to 75]	0 [0 \pm 1]
$\Delta^*(1620) S_{31}$	34 [20 to 30]	-
$\Delta^*(1910) P_{31}$	11 [15 to 30]	-
$N^*(1720) P_{13}$	13 [10 to 20]	38 [4 \pm 1]
$N^*(1520) D_{13}$	67 [55 to 65]	0.10 [0.23 \pm 0.04]
$\Delta(1232) P_{33}$	100 [100]	-
$\Delta^*(1700) D_{33}$	13 [10 to 20]	-

Branching ratios into πN and ηN . The values in brackets are from the PDG, [Amsler et al., PLB 667 (2008)].

Couplings and dressed vertices

Residue a_{-1} vs. dressed vertex Γ vs. bare vertex γ .

◀ back



$$a_{-1} = \frac{\Gamma_d \Gamma_d^{(\dagger)}}{1 - \frac{\partial}{\partial Z} \Sigma}$$

$$g = \sqrt{a_{-1}}$$

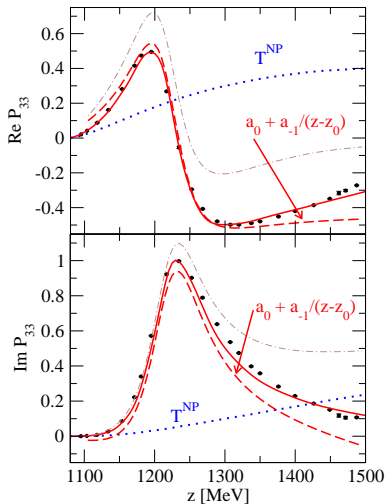
$$r = |(\Gamma_D - \gamma_B)/\Gamma_D|,$$

$$r' = |1 - \sqrt{1 - \Sigma'}|,$$

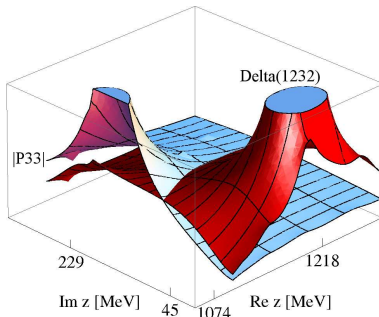
- Dressed Γ depends on T^{NP} .

$$\boxed{\sqrt{a_{-1}} \neq \Gamma \neq \gamma}$$

	γ^C	Γ^C	r [%]	r' [%]
$N^*(1520) D_{13}$	$6.4 - 0.6i$	$13.2 + 1.2i$	53	61
$N^*(1720) P_{13}$	$-0.1 + 5.4i$	$0.9 + 4.8i$	24	45
$\Delta(1232) P_{33}$	$1.3 + 13.0i$	$-2.8 + 22.2i$	45	40
$\Delta^*(1620) S_{31}$	$0.1 + 14.3i$	$5.0 + 5.7i$	130	66
$\Delta^*(1700) D_{33}$	$5.4 - 0.8i$	$6.7 + 1.0i$	33	54
$\Delta^*(1910) P_{31}$	$9.4 + 0.3i$	$1.9 - 3.2i$	222	22



- Poles in T^{NP} may occur \Rightarrow pole repulsion in $T = T^{\text{NP}} + T^{\text{P}}$!



g_{fi} und h_{fi} in JLS-Basis:

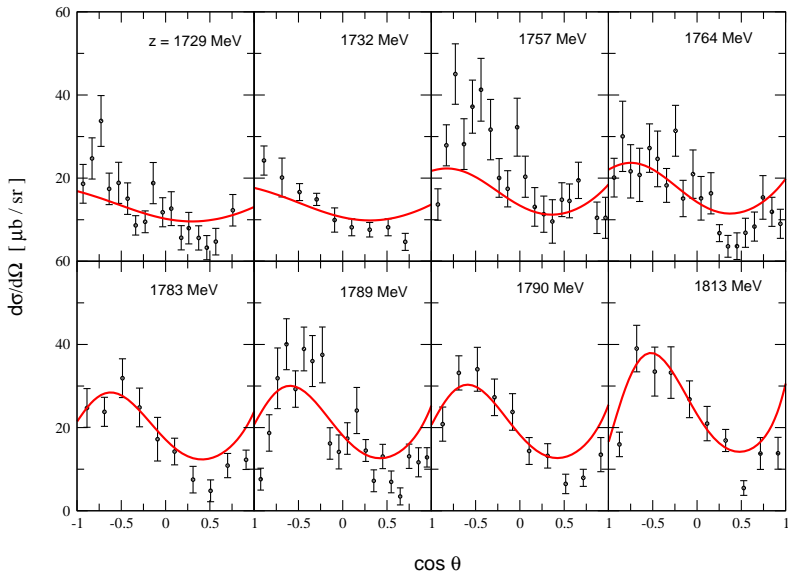
$$g_{fi} = \frac{1}{2\sqrt{k_f k_i}} \sum_j (2j+1) d_{\frac{1}{2}\frac{1}{2}}^j(\theta) \left[\tau^{j(j-\frac{1}{2})\frac{1}{2}} + \tau^{j(j+\frac{1}{2})\frac{1}{2}} \right] \cos \frac{\theta}{2} \\ + \frac{1}{2\sqrt{k_f k_i}} \sum_j (2j+1) d_{-\frac{1}{2}\frac{1}{2}}^j(\theta) \left[\tau^{j(j-\frac{1}{2})\frac{1}{2}} - \tau^{j(j+\frac{1}{2})\frac{1}{2}} \right] \sin \frac{\theta}{2}$$

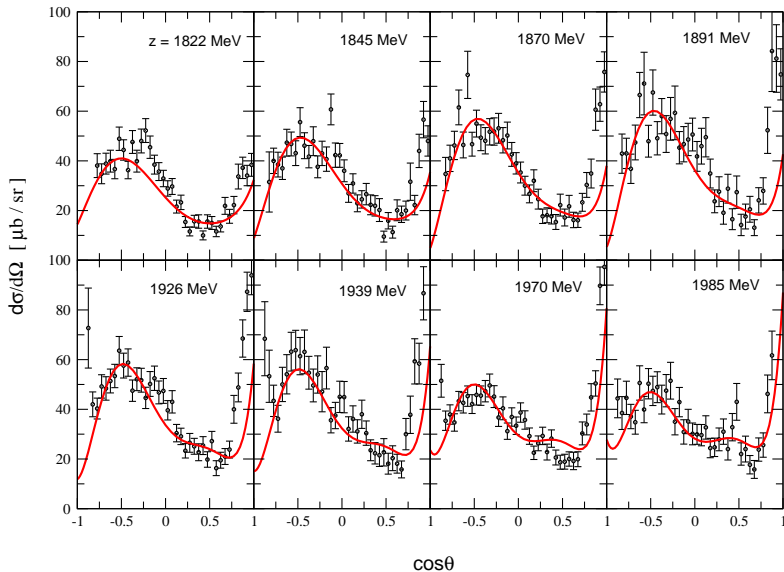
$$h_{fi} = \frac{-i}{2\sqrt{k_f k_i}} \sum_j (2j+1) d_{\frac{1}{2}\frac{1}{2}}^j(\theta) \left[\tau^{j(j-\frac{1}{2})\frac{1}{2}} + \tau^{j(j+\frac{1}{2})\frac{1}{2}} \right] \sin \frac{\theta}{2} \\ + \frac{i}{2\sqrt{k_f k_i}} \sum_j (2j+1) d_{-\frac{1}{2}\frac{1}{2}}^j(\theta) \left[\tau^{j(j-\frac{1}{2})\frac{1}{2}} - \tau^{j(j+\frac{1}{2})\frac{1}{2}} \right] \cos \frac{\theta}{2}$$

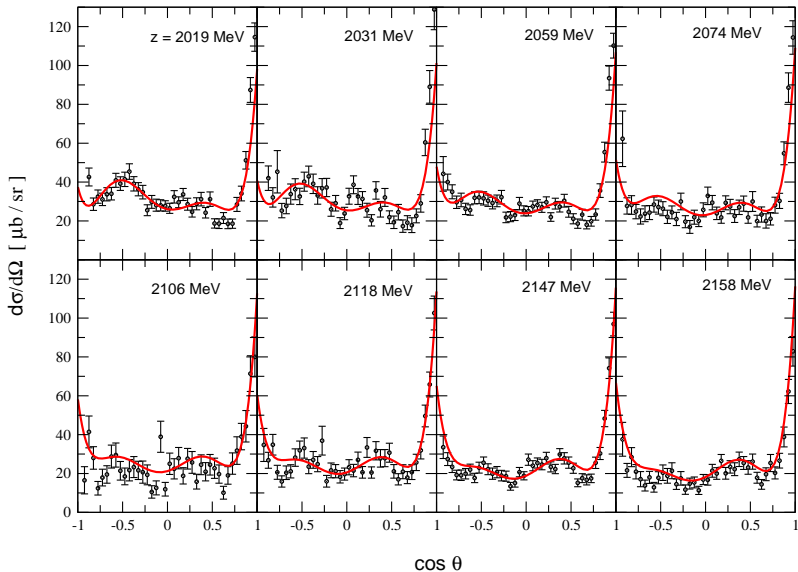
$$\begin{aligned}
 \frac{d\sigma}{d\Omega} &= \frac{k_f}{k_i} (|g_{fi}|^2 + |h_{fi}|^2) \\
 &= \frac{1}{2k_i^2} \frac{1}{2} \cdot \left(\left| \sum_j (2j+1) (\tau^{j(j-\frac{1}{2})\frac{1}{2}} + \tau^{j(j+\frac{1}{2})\frac{1}{2}}) \cdot d_{\frac{1}{2}\frac{1}{2}}^j(\Theta) \right|^2 \right. \\
 &\quad \left. + \left| \sum_j (2j+1) (\tau^{j(j-\frac{1}{2})\frac{1}{2}} - \tau^{j(j+\frac{1}{2})\frac{1}{2}}) \cdot d_{-\frac{1}{2}\frac{1}{2}}^j(\Theta) \right|^2 \right)
 \end{aligned}$$

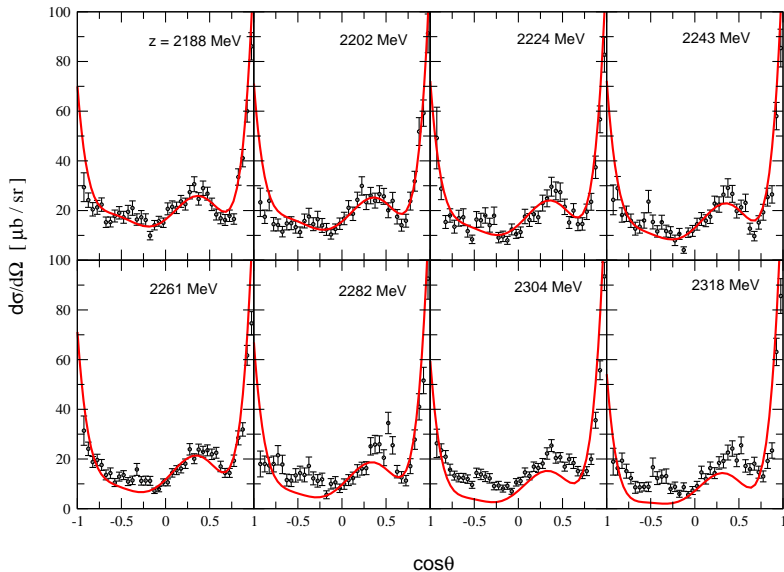
$$\vec{P}_f = \frac{2\text{Re}(g_{fi}h_{fi}^*)}{|g_{fi}|^2 + |h_{fi}|^2} \cdot \hat{n}$$

$$\beta = \arctan \left(\frac{2\text{Im}(h_{fi}^*g_{fi})}{|g_{fi}|^2 - |h_{fi}|^2} \right)$$

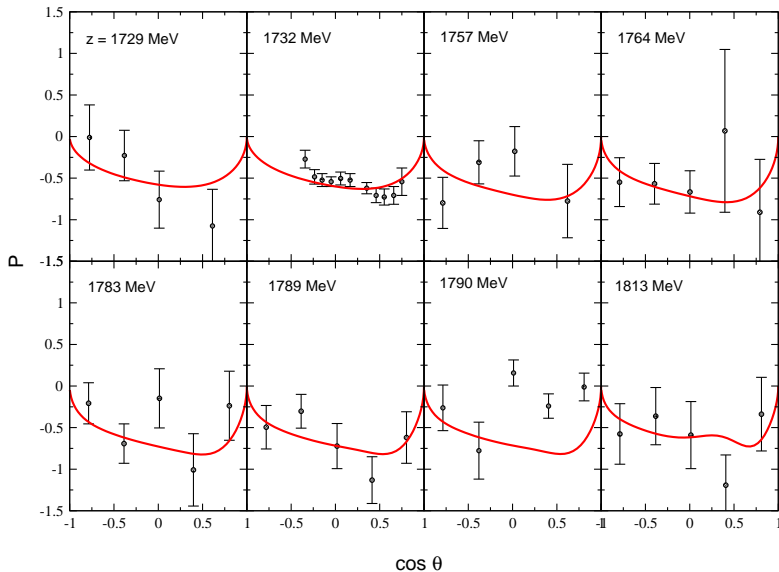




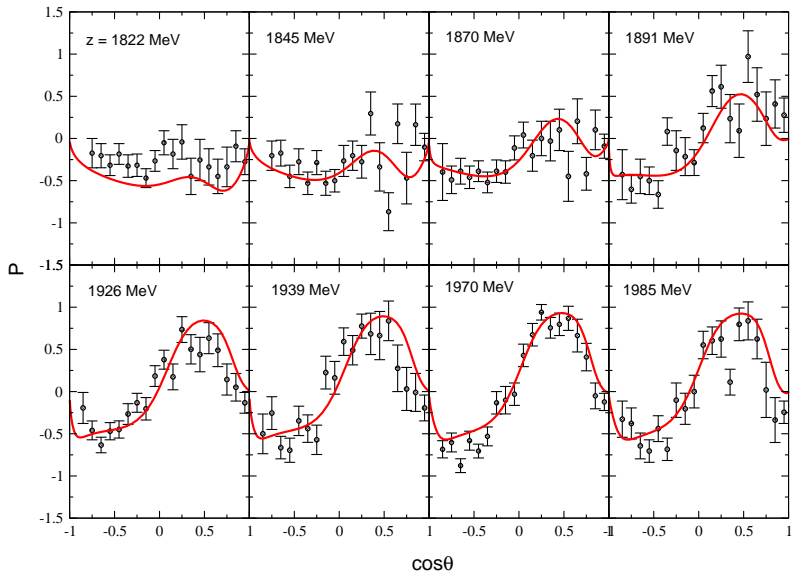




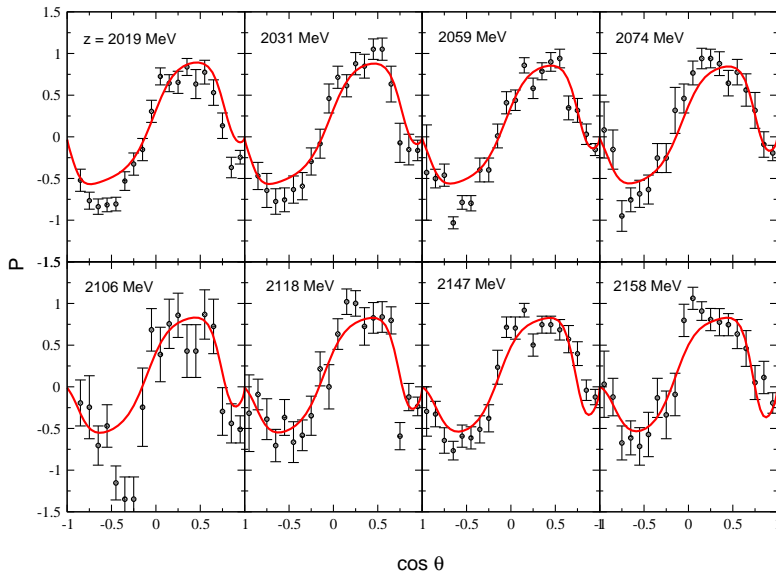
Polarization of $\pi^+ p \rightarrow K^+ \Sigma^+$



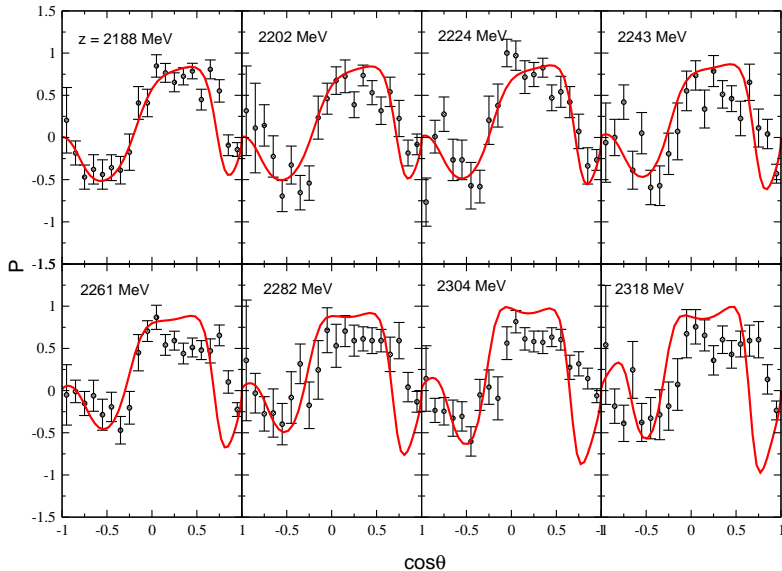
Polarization of $\pi^+ p \rightarrow K^+ \Sigma^+$



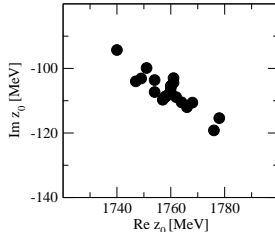
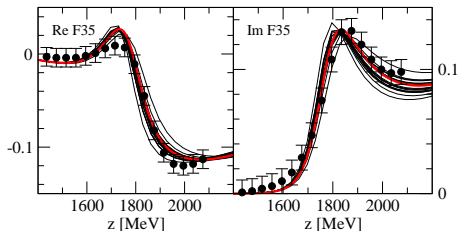
Polarization of $\pi^+ p \rightarrow K^+ \Sigma^+$



Polarization of $\pi^+ p \rightarrow K^+ \Sigma^+$



- Determination of the non-linear parameter error
 - $\chi^2 + 1$ criterion.
 - Varying 39 of 40 parameters to get parameter error.
- Get error on derived quantities like pole positions and residues.
- So far, simplified consideration (error from πN not available, because energy dependent GWU/SAID solution is fitted [PRC74 (2006)]).



Error estimates for parameters and derived quantities

Table: Error estimates of bare mass m_b and bare coupling f for the $\Delta(1905)F_{35}$ resonance.

m_b [MeV]	πN	ρN	$\pi\Delta$	ΣK
2258_{-43}^{+44}	$0.0500_{-0.0012}^{+0.0011}$	$-1.62_{-1.61}^{+1.29}$	$-1.15_{-0.022}^{+0.030}$	$0.120_{-0.0059}^{+0.0065}$

Table: Error estimates of pole position and residues for the $\Delta(1905)F_{35}$ resonance.

			$\pi N \rightarrow \pi N$	$\pi N \rightarrow K\Sigma$
Re z_0 [MeV]	1764_{-20}^{+18}	$ r $ [MeV]	$11_{-1.4}^{+1.7}$	$1.4_{-0.21}^{+0.24}$
Im z_0 [MeV]	-109_{-12}^{+13}	θ [$^\circ$]	$-45_{-11}^{+3.8}$	$-313_{-10}^{+4.2}$

	Re z_0 [MeV]	$ r $ [MeV]	$(\Gamma_{\pi N}^{1/2} \Gamma_{K\Sigma}^{1/2}) / \Gamma_{\text{tot}}$ [%]		
	-2 Im z_0 [MeV]		θ [$^\circ$]	This study	Candlin (1983)
$\Delta(1905) F_{35}$	1764	1.4	1.23	1.5(3)	<1
5/2 ⁺ ****	218	-313			
$\Delta(1910) P_{31}$	1721	5.5	2.98	<3	1.1
1/2 ⁺ ****	323	-6			
$\Delta(1920) P_{33}$	1884	5.9	5.07	5.2(2)	2.1(3)
3/2 ⁺ ***	229	-38			
$\Delta(1930) D_{35}$	1865	1.6	2.14	<1.5	
5/2 ⁻ ***	147	-43			
$\Delta(1950) F_{37}$	1873	2.7	2.54	5.3(5)	—
7/2 ⁺ ****	206	-255			

Coupled channels and gauge invariance

Haberzettl, PRC56 (1997), Haberzettl, Nakayama, Krewald, PRC74 (2006),

← back

Hadronic scattering:

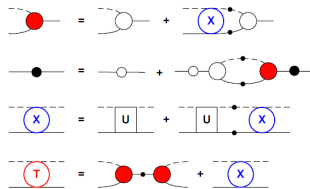
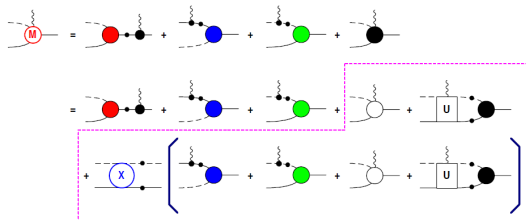


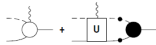
Photo-production:



Gauge invariance: Generalized Ward-Takahashi identity (WTI)

(Note the condition of current conservation $k_\mu M^\mu = 0$ is necessary but not sufficient!)

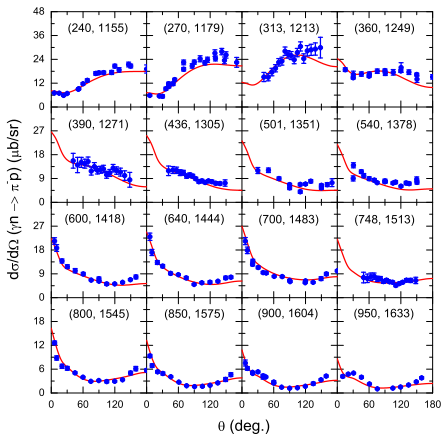
$$k_\mu M^\mu = -|F_s \tau\rangle S_{p+k} Q_i S_p^{-1} + S_{p'}^{-1} Q_f S_{p'-k} |F_u \tau\rangle + \Delta_{p-p'+k}^{-1} Q_\pi \Delta_{p-p'} |F_t \tau\rangle$$

Strategy: Replace  by phenomenological contact term such that the generalized WTI is satisfied

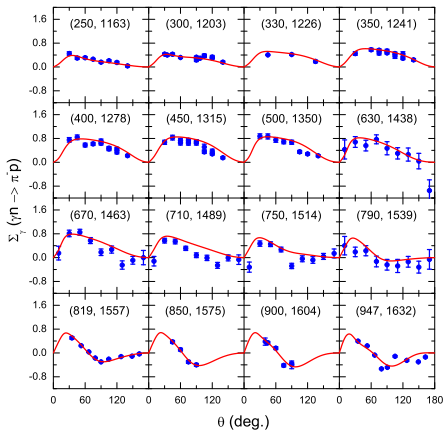
$d\sigma/d\Omega$ and Σ_γ for $\gamma n \rightarrow \pi^- p$

preliminary

◀ back



Differential cross section for $\gamma n \rightarrow \pi^- p$

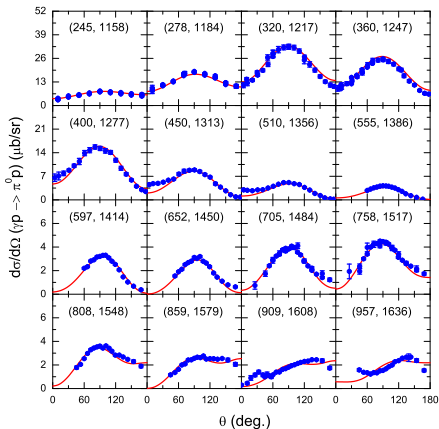


Photon spin asymmetry for $\gamma n \rightarrow \pi^- p$

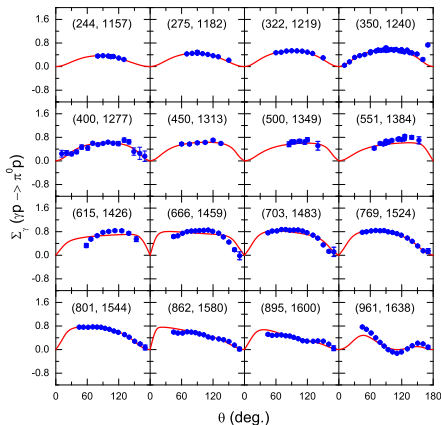
$d\sigma/d\Omega$ and Σ_γ for $\gamma p \rightarrow \pi^0 p$

preliminary

◀ back



Differential cross section for $\gamma p \rightarrow \pi^0 p$



Photon spin asymmetry for $\gamma p \rightarrow \pi^0 p$

Discretization of momenta in the scattering equation:

$$T(q'', q') = V(q'', q') + \int_0^\infty dq q^2 V(q'', q) \frac{1}{z - E_1(q) - E_2(q) + i\epsilon} T(q, q')$$

$$\int \frac{\vec{d}^3 q}{(2\pi)^3} f(|\vec{q}|^2) \rightarrow \frac{1}{L^3} \sum_{\vec{n}_i} f(|\vec{q}_i|^2), \quad \vec{q}_i = \frac{2\pi}{L} \vec{n}_i, \quad \vec{n}_i \in \mathbb{Z}^3$$

$$T(q'', q') = V(q'', q') + \frac{2\pi^2}{L^3} \sum_{i=0}^\infty \vartheta(i) V(q'', q_i) \frac{1}{z - E_1(q_i) - E_2(q_i)} T(q_i, q'),$$

- Can be also expressed in terms of the Lüscher \mathcal{Z}_{00} function up to e^{-L} relativistic corrections.
- Takes into account discretization effects of the potentials themselves.
- Twisted boundary conditions, e.g.

$$u(\mathbf{x} + L\mathbf{e}_i) = u(\mathbf{x}), \quad d(\mathbf{x} + L\mathbf{e}_i) = d(\mathbf{x}), \quad s(\mathbf{x} + L\mathbf{e}_i) = e^{i\theta} s(\mathbf{x}),$$

especially suited for coupled-channels problem (enables to move thresholds) [V. Bernard, M. Lage, U.-G. Meißner, A. Rusetsky, JHEP (2011)].

